

Realization of *p*-Type Conductivity in ZnO via Potassium Doping

M. BOUSMAHA^{a,*}, M.A. BEZZEROUK^a, R. BAGHDAD^a, K. CHEBBAH^a, B. KHARROUBI^a
AND B. BOUHAFS^b

^aDepartment of Physics, Faculty of Material Sciences, Ibn Khaldoun University — Tiaret,
BP 78, Zaaroura Road, 14000 Tiaret, Algeria

^bModeling and Simulation in Materials Science Laboratory, Physics Department, University of Sidi Bel-Abbès,
Sidi Bel Abbès 22000, Algeria

(Received December 27, 2015; revised version April 23, 2016; in final form May 19, 2016)

Our work focuses on the study of the electronic structure of undoped and K-doped ZnO using density functional theory as implemented in the Wien2k package. Generalized gradient approximation and GGA plus Tran–Blaha–modified Becke–Johnson (TB-mBJ) were used to calculate the exchange–correlation energy. From the electronic properties, ZnO has a direct band gap in ($\Gamma - \Gamma$) direction with a value of 0.76 eV within GGA and 2.63 eV within GGA + TB-mBJ. For the K-doped ZnO (12.5%) the gap was found to be 1.15 eV within GGA and 3.28 eV within GGA + TB-mBJ, we have observed that an emersion of a new narrow band exists in the valence band which is mainly caused by K 3*p* states with a little Zn 4*s* and Zn 3*d* effect.

DOI: [10.12693/APhysPolA.129.1155](https://doi.org/10.12693/APhysPolA.129.1155)

PACS/topics: 63.20.dk, 81.05.Dz, 73.20.At

1. Introduction

ZnO is a II–VI binary compound semiconductor with a wide direct band gap of 3.37 eV at room temperature and a large exciton binding energy of 60 meV that makes ZnO a promising material for possible applications such as optoelectronic devices, high efficiency lasers operable at room temperature and light emitting diodes [1–4]. However, the development of such optoelectronic devices has been greatly impeded by the fact that *p*-*n* homojunction of ZnO is extremely difficult to fabricate, because pure ZnO with a wurtzite structure occurs naturally as *n*-type semiconductors, and the realization of *p*-type ZnO is rather difficult. Group I elements (Li, Ag, Na, K) substituting for Zn are one main class of candidate for *p*-type doping [5–8]. Park et al. [7] found that substitutional group-I elements are shallow acceptors. In the absence of compensation by intrinsic defects, the most likely reason for doping difficulty is the formation of interstitials for group-I elements. Ping et al. have found that *p*-type ZnO can be realized through codoping by N and B [9]. The realization of *p*-type Ag-doped ZnO thin films has been reported [10, 11]. In other previous studies [12–14], growth of *p*-type ZnO doped with Na was achieved using pulsed laser deposition method. Electroluminescence emission from ZnO based light emitting diodes with Na doping as the *p*-type layer was observed. The results showed that Na can behave as a good acceptor in ZnO and can provide even higher hole concentration. P-doped *p*-type ZnO thin films were successfully fabricated

by Su et al. [15]. Doping ZnO with Al also gives *p*-type thin films deposited on *n*-Si substrate [16]. For the K-doped ZnO, Huang et al. [17] showed a conversion of conductivity from *n*-type to *p*-type when the K content reaches 6%.

Motivated by these theoretical and experimental reports on the *p*-type ZnO doped with group-I elements, we have studied the electronic properties of pure and K-doped ZnO using first-principles calculations based on density functional theory (DFT) to describe the possible achieving *p*-type ZnO by K doping.

2. Computational method

We have performed the *ab initio* calculations using the full potential linearized augmented plane wave (FPLAPW) method within the DFT, as implemented in the WIEN2k program package [18]. The exchange and correlation effects were treated within the generalized gradient approximation (GGA) [19] and generalized gradient approximation plus Tran–Blaha modified Becke–Johnson (TB-mBJ) [20]. The mBJ approximation was used to calculate electronic properties, exactly the band gap that can be found in better agreement with the experimental band gap. In our calculations, we expanded the basis functions up to $R_{\text{MT}}K_{\text{max}} = 8$, where R_{MT} is the smallest of all atomic sphere radii and K_{max} is the plane wave cut-off. The self-consistent calculation was considered to be stable when the total energy convergence is less than 10^{-5} Ry. The electronic structure studies on K-doped ZnO are based on the $\text{Zn}_{1-x}\text{K}_x\text{O}$ ($x = 0.125$) using a $2 \times 2 \times 1$ supercell of ZnO which was performed by substituting one Zn atom with one K atom (Fig. 1). According to Ref. [21], the wurtzite ZnO has a hexagonal crystal (space group $P63mc$, $a = b = 3.25$ Å, $c = 5.21$ Å, and $\alpha = \beta = 90^\circ$, $\gamma = 120^\circ$).

*corresponding author; e-mail: mhbousmaha@gmail.com

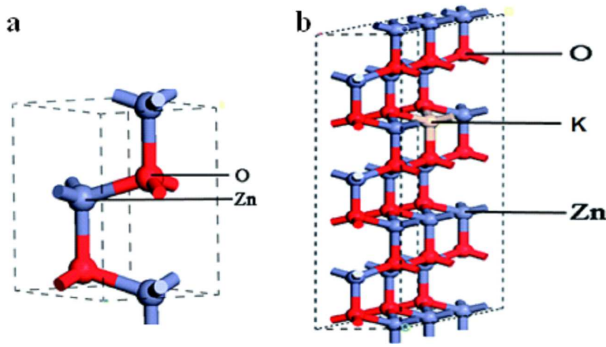


Fig. 1. The $1 \times 1 \times 1$ unit cell of pure ZnO (a) and $2 \times 2 \times 1$ supercell of K doped ZnO (b).

3. Results and discussion

3.1. Undoped ZnO

The electronic band structure of pure ZnO is shown in Fig. 2, where the Fermi level has been specified to be 0 eV [22]. The direct band gap by GGA is 0.76 eV at a highly symmetric point (sigma Γ), which is in good agreement with other theoretical calculations [23–25], but lower than the experiment value of 3.37 eV due to the limitation of DFT in GGA, and the discontinuity in the exchange–correlation potential is not taken into account in the framework of DFT [26]. However, the band gap obtained by GGA + TB-mBJ approximation is 2.63 eV, which is close to the experimental value and in good agreement with the theoretical value of 2.6 eV found by Abbassi et al. [27].

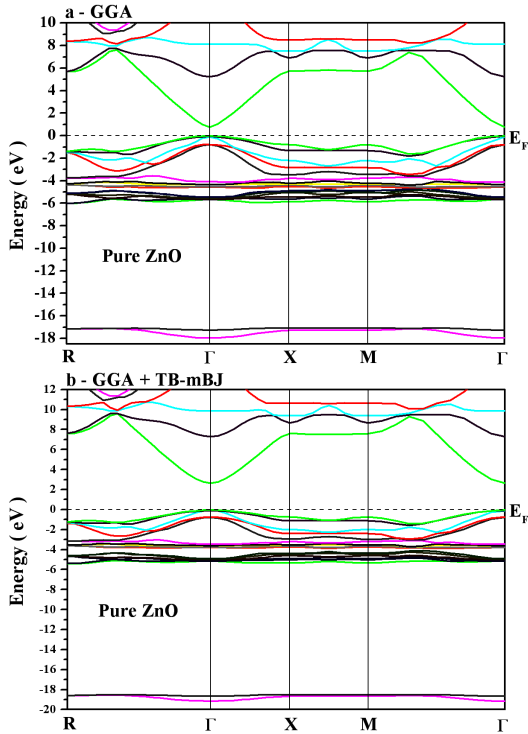


Fig. 2. Electronic band structure of pure ZnO within GGA (a) and GGA + TB-mBJ (b).

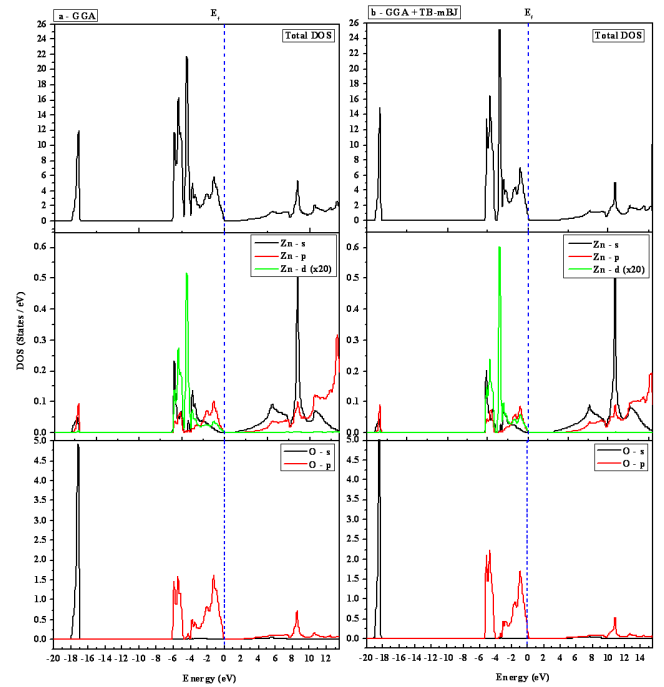


Fig. 3. Total and partial density of states of pure ZnO within GGA (a) and GGA + TB-mBJ (b).

The total density of states (TDOS) of undoped ZnO and the partial density of states (PDOS) of O and Zn atoms are shown in Fig. 3, where the valence band is represented by VB, and the conduction band is denoted by CB. The Fermi level indicated by a dashed line is set as zero which is the highest occupied state. It can be seen that the lower valence band from mainly Zn 3d changes gently because the 3d states of Zn are full of electrons and the Fermi level of the unit cell of pure ZnO is at the top of the valence band. The valence band maximum and the conduction band minimum are mainly dominated by O 2p and Zn 4s states, respectively, which is also proved by experimental results [28, 29]. We can see also that the valence band mainly consists of a mixture of the 3d states of Zn and the 2p, 2s states of O. The upper valence band is mainly composed of O 2p states between -5.32 and 0.16 eV by GGA and between -5.57 and 0.16 eV by GGA + TB-mBJ with a small contribution from Zn 3d states, while the O 2s states become visible in the range from -16.86 to -15.91 eV and from -19.34 to -18.33 eV (respectively within GGA and GGA + TB-mBJ), which corresponds to the two bands in Fig. 2. The conduction band of undoped ZnO is mainly composed of O 2p and Zn 2s states. The results above are in good agreement with other reports [30, 31].

3.2. P-type K-doped ZnO

The electronic band structure of K-doped ZnO along the symmetry points in the first Brillouin zone was represented in Fig. 4. The calculated direct band gap by GGA is 1.15 eV and 3.28 eV with GGA + TB-mBJ approximation. In comparison with pure ZnO, the value of band

gap of K doped ZnO becomes larger than the first one. New bands appeared in the valence band exactly in the region between -9.75 eV and -9.23 eV with GGA and between -10.14 eV and -9.65 eV with GGA + TB-mBJ potential which causes a deviation of the Fermi level into the valence band, so from this reason we can say that the K doped ZnO has a *p*-type character. The curvature becomes more flat indicating an increase of the effective mass of holes in the valence band. Potassium can be considered as a good acceptor in ZnO, and can offer even higher hole concentration.

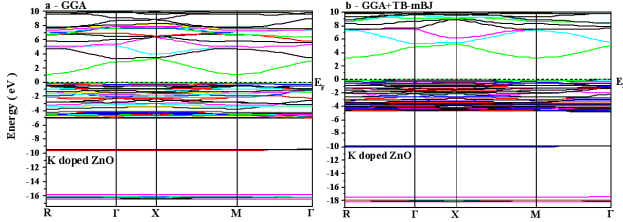


Fig. 4. Electronic band structure of K doped ZnO within GGA (a) and GGA + TB-mBJ (b).

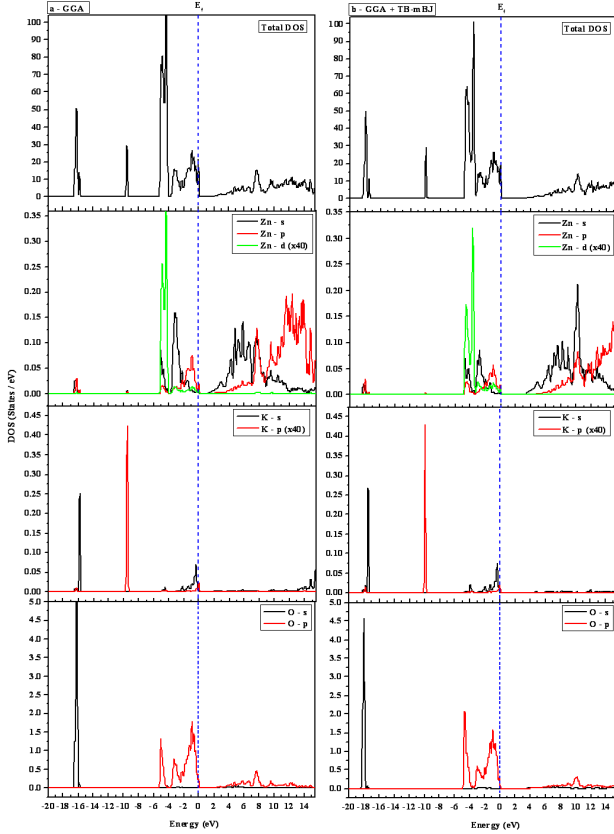


Fig. 5. Total and partial density of states of K doped ZnO within GGA (a) and GGA + TB-mBJ (b).

Figure 5 shows the TDOS of K-doped ZnO and the PDOS of Zn, K and O atoms. Compared with DOS of undoped ZnO in Fig. 3, it is apparent that the introduction of K atom changes the structures

by a considerable amount. We can see that a new narrow band exists at -9.5 eV and -9.92 eV (respectively with GGA and GGA + TB-mBJ) with weak contribution with other bands, which is mainly caused by K *3p* states with a little Zn *4s* and Zn *3d* effect which shows that K *3p*, Zn *4s*, and Zn *3d* have coupling effect. This phenomenon can be explained by the appearance of more electrons in the valence band moving toward the higher energy region. Furthermore, the Fermi-level of K-doped ZnO shifts downward into the valence band as shown in Fig. 6. This shift originates mainly from K *3p* states with a little contribution from Zn *3p*, Zn *3d*, and O *2p* states. These results indicate that *p*-type ZnO can be achieved by K doping.

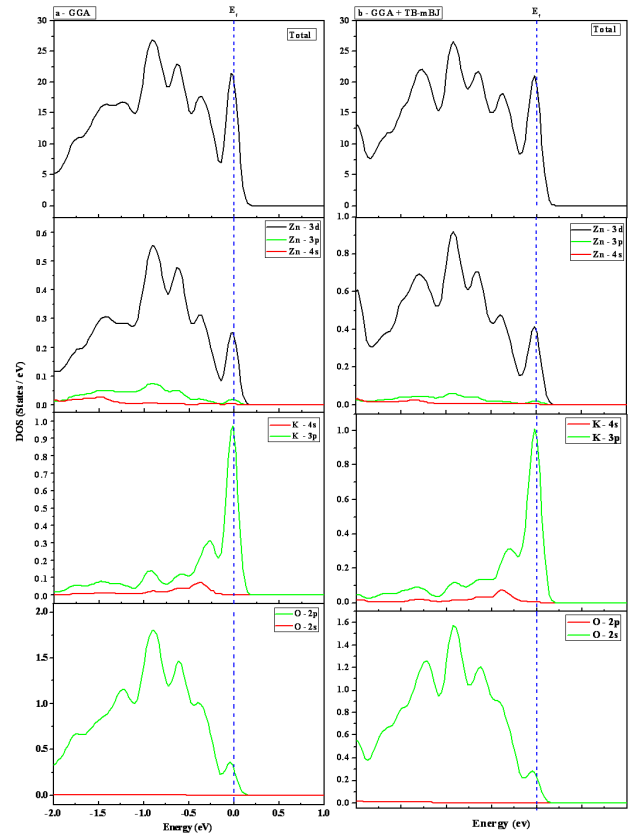


Fig. 6. Total and partial density of states of K-doped ZnO near the Fermi level within GGA (a) and GGA + TB-mBJ (b).

4. Conclusion

In summary, electronic properties of pure and K-doped ZnO were studied using first principles calculations within GGA and GGA + TB-mBJ approximation. Both electronic band structures and density of states showed an appearance of a new narrow band in the valence band and the Fermi level shifts towards the valence band which indicates that *p*-type ZnO can be achieved by K doping. All these characteristics made K-doped ZnO useful semiconductor for optoelectronic devices application.

References

- [1] D.M. Bagnal, Y.F. Chen, Z. Zhu, T. Yao, S. Koyama, M.Y. Shen, T. Goto, *Appl. Phys. Lett.* **70**, 2230 (1997).
- [2] Z.K. Tang, G.K.L. Wong, P. Yu, M. Kawasaki, A. Ohtomo, H. Koinuma, Y. Segawa, *Appl. Phys. Lett.* **72**, 3270 (1998).
- [3] D.K. Hwang, S.H. Kang, J.H. Lim, E.J. Yang, J.Y. Oh, J.H. Yang, S.J. Park, *Appl. Phys. Lett.* **86**, 222101 (2005).
- [4] M. Willander, O. Nur, Q.X. Zhao, L.L. Yang, M. Lorenz, B.Q. Cao, J. Zúñiga Pérez, C. Czekalla, G. Zimmermann, M. Grundmann, A. Bakin, A. Behrends, M. Al-Suleiman, A. El-Shaer, A.C. Mofor, B. Postels, A. Waag, N. Boukos, A. Travlos, H.S. Kwack, J. Guinard, D.L.S. Dang, *Nucl. Technol.* **20**, 332001 (2009).
- [5] P.H. Kasai, *Phys. Rev.* **130**, 989 (1963).
- [6] O.F. Schirmer, *J. Phys. Chem. Solids* **29**, 1407 (1968).
- [7] C.H. Park, S.B. Zhang, S.H. Wei, *Phys. Rev. B* **66**, 073202 (2002).
- [8] E.C. Lee, K.J. Chang, *Physica B* **376–377**, 707 (2006).
- [9] L. Ping, D.S. Hua, Z.X. Yong, Z. Li, L.G. Hong, Y.J. Ying, *Commun. Theor. Phys.* **54**, 723 (2010).
- [10] L.J. Sun, J. Hu, H.Y. He, X.P. Wu, X.Q. Xu, B.X. Lin, Z.X. Fu, B.C. Pan, *Solid State Commun.* **149**, 1663 (2009).
- [11] F.J. Lugo, H.S. Kim, S.J. Pearton, C.R. Abernathy, B.P. Gila, D.P. Norton, Y.L. Wang, F. Ren, *Electrochem. Solid State Lett.* **12**, H188 (2009).
- [12] S.S. Lin, J.G. Lu, Z.Z. Ye, H.P. He, X.Q. Gu, L.X. Chen, J.Y. Huang, B.H. Zhao, *Solid State Commun.* **148**, 25 (2008).
- [13] S.S. Lin, H.P. He, Y.F. Lu, Z.Z. Ye, *J. Appl. Phys.* **106**, 093508 (2009).
- [14] S.S. Lin, Z.Z. Ye, J.G. Lu, H.P. He, L.X. Chen, X.Q. Gu, J.Y. Huang, L.P. Zhu, B.H. Zhao, *J. Phys. D Appl. Phys.* **41**, 155114 (2008).
- [15] S.C. Su, X.D. Yang, C.D. Hu, *Physica B* **406**, 1533 (2011).
- [16] H.J. Jin, M.J. Song, C.B. Park, *Physica B* **404**, 1097 (2009).
- [17] Y. Huang, W. Zhou, P. Wu, *Solid State Commun.* **183**, 31 (2014).
- [18] P. Blaha, K. Schwarz, P. Sorantin, S.K. Trickey, *Comput. Phys. Commun.* **59**, 339 (1990).
- [19] J.P. Perdew, K. Burke, M. Ernzerhof, *Phys. Rev. Lett.* **77**, 3865 (1996).
- [20] F. Tran, P. Blaha, *Phys. Rev. Lett.* **102**, 226401 (2009).
- [21] R. Baghdad, B. Kharroubi, A. Abdiche, M. Bousmaha, M.A. Bezzerrouk, A. Zeinert, M. El Marssi, K. Zellama, *Superlatt. Microstruct.* **52**, 711 (2012).
- [22] Q. Hou, J. Li, C.W. Zhao, C. Ying, Y. Zhang, *Physica B* **406**, 1956 (2011).
- [23] C. Zuo, J. Wen, S. Zhu, C. Zhong, *Opt. Mater.* **32**, 595 (2010).
- [24] A. Schleife, F. Fuchs, J. Furthmüller, F. Bechstedt, *Phys. Rev. B* **73**, 245212 (2006).
- [25] K. Osuch, E.B. Lombardi, W. Gebicki, *Phys. Rev. B* **73**, 075202 (2006).
- [26] R.W. Godby, M. Schlüter, L.J. Sham, *Phys. Rev. B* **37**, 10159 (1988).
- [27] A. Abbassi, H. Ez-Zahraouy, A. Benyoussef, *Opt. Quant. Electron.* **47**, 1869 (2015).
- [28] W. Ranke, *Solid State Commun.* **19**, 685 (1976).
- [29] Y. Yan, J. Li, S.H. Wei, M.M. Al-Jassim, *Phys. Rev. Lett.* **98**, 135506 (2007).
- [30] Y. Imai, A. Watanabe, I. Shimono, *J. Mater. Sci. Mater. Electron.* **14**, 149 (2003).
- [31] Y. Shen, L. Mi, X. Xu, J. Wu, P. Wang, Z. Ying, N. Xu, *Solid State Commun.* **148**, 301 (2008).